Combinatorics and Modelling of Highly Branched Polymers

Jason Palin

A thesis submitted to the Faculty of Graduate Studies in partial fulfillment of the requirements for the degree of Master of Arts

Graduate Program in Mathematics and Statistics York University
Toronto, Ontario

August 2025

Abstract

Highly branched polymers such as dendrimers and hyperbranched polymers have a found a variety of chemical applications owing to their unique structural and functional properties, but in many cases are still lacking sufficient theoretical characterization. This thesis takes marginal steps toward addressing this by firstly studying a combinatorial analog of the Degree of Branching - a quantity used by chemists to classify the extent of branching in polymers - in the mathematically convenient setting of lattice models of polymers. Next the adsorption behaviour of dendrimers is studied by adapting the Monte Carlo method of Random Sequential Adsorption to dendrimers and applying the model to experimental results of a novel synthetic dendrimer of interest.

Acknowledgements

Thank you to my supervisor, Professor Neal Madras, for his extensive guidance and his patience in providing it. Thank you also to Professors Ozzy Mermut and Christopher J. Barrett for their support.

Contents

List of Figures

1 Introduction

Polymers are a broad class of molecules consisting of repeating molecular subunits, called monomers, attached to each other through covalent bonds. The composition of polymers lends them to a fantastic variety of applications in the physical sciences and engineering, wherein by using different monomers and attaching them in different fashions, molecules can be constructed with a huge variety of specific structures, properties, and applications [26]. Rubber, silk, and DNA are all examples of naturally occurring polymers. Nylon, polystyrene, and polyester are all examples of synthetic (human made) polymers.

Owing to the variety of polymerization processes by which monomers are combined into a polymer, polymers can take on a variety of shapes (see [25] Ch. 1 for a survey of common polymer architecture). When monomers attach one-by-one in a chain like fashion they form a rope-like structure called a linear polymer. Many polymerization processes can also cause 2 or more additional monomers to be attached to a growing polymer, causing branching behaviour [26].

The wide variety of mechanisms for branching and the degree to which this branching is restrained produce different classes of branched polymers. Dendrimers are a kind of branched polymer with a spherically symmetric shape and regular branching behaviour created by a slow and controlled polymerization process. Hyperbranched polymers are another class of polymers with a high extent of branching, but asymmetrical and with irregular branching patterns.

Polymers which have a significant amount of branching exhibit distinct functions, physical characteristics [17], and rheological properties [8]. In this thesis we will examine modelling of highly-branched polymers at a highly general level of lattice models of polymers, and at a highly specific level of modelling informed by a particular dendrimer of interest - dendritic polyglycerol amine. We now turn to introducing both of these.

1.1 Lattice models of Polymers

Mathematically, the repeating and frequently identical subunits of polymers allow for crude representations of them via well-studied combinatorial objects such as random and self avoiding walks [23] [21].

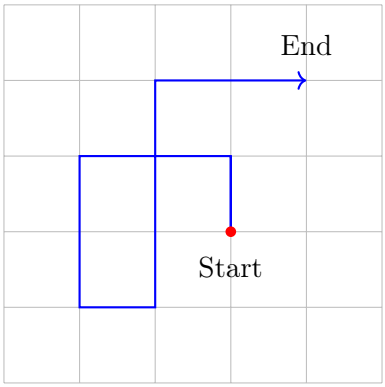

Figure 1.1: An example random walk in $\mathbb{Z}^2$ consisting of 11 steps.

A (lattice) random walk is a discrete-time stochastic process on a lattice with characteristic length b where at every time step a step of length b is taken from the current location of the walk to any of the adjacent lattice points with uniform probability. A typical example for polymer modelling is a random walk on a grid or hypercubic lattice $\mathbb{Z}^d$. Fig. 1.1 displays an example of a random walk on $\mathbb{Z}^2$.

Since steps in a random walk are allowed to intersect with previously taken steps, random walks are Markovian, meaning the location of each step of a random walk depends only on the step preceding it [20]. This simplifies their analysis and allows for exact formulas of many key properties such as the total amount of distinct random walks of N steps and the probability of a random walk being at some point after N steps. Such exact formulas are particularly useful in polymer modelling where they can be used as inputs in formulas involving size distribution and entropy [17].

However, the allowance for self-intersection of random walks which makes the process Markovian is only a good physical assumption when the polymers are "ideal" - meaning that interactions between monomers sufficiently separated in a polymer can be ignored. For most polymers and solvents such an assumption is not sound; monomers have a so-called excluded volume surrounding them where spatial overlap with the rest of the polymer chain becomes highly unlikely.

In such a case, the corrected replacement to random walks is the self-avoiding walk (SAW), which proceeds similarly as the random walk but now forbids steps to points of the lattice which have already been visited by the walk (see Fig. 1.2).

The trade off for greater realism in polymer modelling in SAWs is that they are manifestly

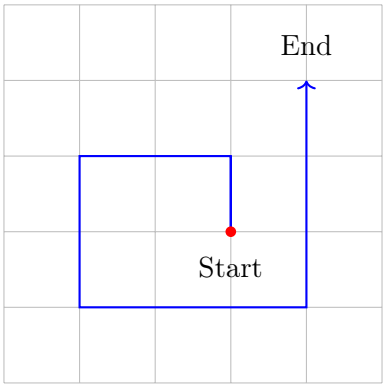

Figure 1.2: An example self-avoiding walk in $\mathbb{Z}^2$ consisting of 11 steps.

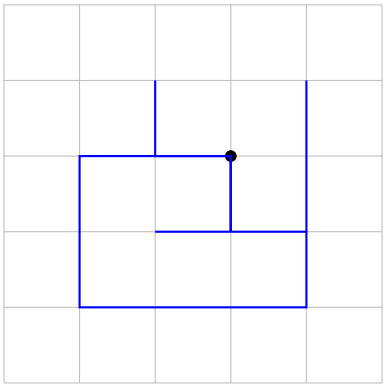

Figure 1.3: An example lattice animal in $\mathbb{Z}^2$.

non-Markovian. Many key properties of SAWs such as enumeration of the amount of SAWs of N steps are only known for low N and generally determined by numerical or asymptotic methods [15].

Both random and self-avoiding walks have another limitation: as 'walks' they only model polymers which have a linear structure. Many key polymers (such as the particular polymers of interest in this thesis) have a structure that involves branching. The most general lattice-based model is that of a lattice animal, which is simply a connected graph with vertices on lattice points and edges between adjacent vertices. A lattice animal can represent the ideal state of a branched polymer, where no restrictions are placed on self intersection.

The analog of self-avoiding walks for the branched case is given by a lattice tree - the primary combinatorial objects of interest in this paper. A lattice tree is an *acyclic* lattice animal, meaning that if we start from any vertex on a lattice tree, we cannot find a path along the edges of that tree starting from that vertex that returns to that vertex without traversing the same edge twice (see Fig. 1.4).

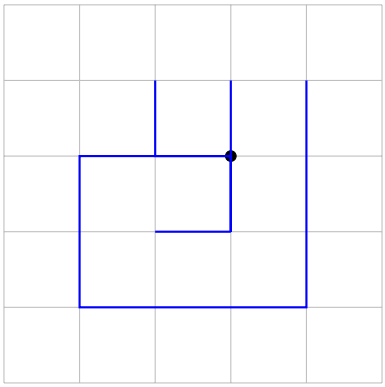

Figure 1.4: An example lattice tree in $\mathbb{Z}^2$

Both lattice animals and lattice trees are not constructed by a 'walk' process as in random walks and self-avoiding walks, and hence do not have a start or end point. They are required to have at least one vertex at the origin, which makes the class of lattice trees or animals of a fixed amount of vertices finite.

The level of abstraction in lattice trees (as well as in all the other lattice based models described above) means that they can be put toward a wide array of polymer modelling problems. One particular class of such problems is that of modelling polymer adsorption: the process of a polymer becoming attached to a surface.

In the context of lattice models, the surface is typically taken as a hyperplane, and adsorbed polymers are lattice trees with at least one vertex contained in the hyperplane. In two dimensions, for instance, the surface could be taken to be the line $x = 0$, and the class of polymers considered would be trees which have at least one vertex along $x = 0$, up to translational equivalence in the y direction (see Fig. 1.5). In three dimensions the surface would be a plane, such as $z = 0$, and trees with at least one vertex along this plane would be considered up to translational equivalence in the x and y directions.

In this thesis, our focus is on polymers which exhibit a high amount of branching behaviour. A quantitative measure of the extent of branching in a polymer sometimes employed by experimentalists is that of the *degree of branching* (DB) of a polymer.

The DB of a polymer is defined following [26] to be

$$DB = (D_d + D_t)/D \tag{1.1}$$

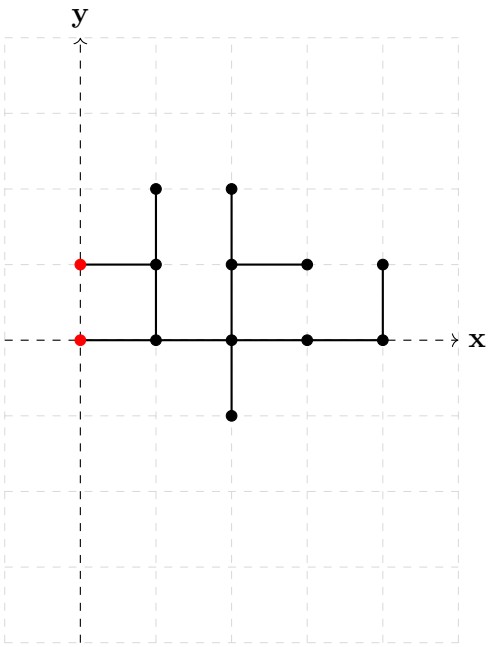

Figure 1.5: Example of a tree with two adsorbed sites, represented by red coloured vertices, in $\mathbb{Z}^2$.

where

D_d = The number of dendritic monomers, i,e. monomers with at least three others attached.

D_t = The number of terminal monomers, i.e. monomers lying at the ends of chains of polymers.

D_L = The number of linear monomers, i.e. monomers attached to two other monomers.

D = The total number of monomers $(D_d + D_t + D_L)$.

The DB can be used as a rough means of classifying well-known species of branched polymers [25]. Dendrimers, a class of polymers with a highly regular pattern of branching typically have a DB close to 1. Hyperbranched polymers, which display much more irregular branching, typically have a DB between 0.4 and 0.6 [10].

It is immediately evident from the definition of DB that it can be extended to lattice tree models of branched polymers. Let τ be a lattice tree in $\mathbb{Z}^n$, and let

- D_d := The number of dendritic vertices of τ, i.e. vertices with degree $\deg(v) \geq 3$
- D_t := The number of terminal vertices of τ, i.e. vertices with degree $\deg(v) = 1$
- D_L := The number of linear vertices of τ, i.e. vertices with degree $\deg(v) = 2$

- $D :=$ The total number of vertices of τ, i.e. $D_d + D_t + D_L$.

To restrict ourselves to polymers which have a significant extent of branching, we pick a somewhat arbitrary convenient threshold of DB which physically includes dendrimers and more highly-branched species of hyperbranched polmers. More precisely, we say that τ is an HB (Highly-Branched) tree if it holds that

$$DB := \frac{D_d + D_t}{D} \geq 0.5. \tag{1.2}$$

Investigating analogs of properties and results for lattice tree models of polymers in the case of HB trees will be the focus of chapter two of this thesis. As HB trees have not been previously studied, the results in this chapter are all novel. Many of the results such as the proof of supermultiplicativity of the class of HB trees and the adsorption results adapt techniques and results developed for general lattice trees.

1.2 Dendritic Polyglycerol Amine

Neuronal cell culture, the technique of growing neurons cells outside of their native environment in the human nervous system, expectedly fosters much important neuroscientific research. Neurons require the support of biological substrates (such as astroglial cells within the human brain [4]) in order to properly grow and survive. A recent synthetic polymer which has demonstrated very promising results as a functional substrate for growing neural cell culture is dendritic polyglycerol amine (dPGA) [7].

The dPGA structure (see Figure 1.6) consists of a hyperbranched polyglycerol molecule with some fraction of branch ends populated by amine groups. Polyglycerol is a structure formed by many attachments of a molecule called glycerol, which serves as the monomer here. Amine groups are NH_2 molecules at the ends of the dendrimer. Hyperbranched polyglycerol is a well known branched polymer which typically has DB around 0.5 - 0.6 and is used for its flexible structure and ease of polymerization [1]. Amine groups (which become positively charged when placed in acid, as is the case for solvents dPGA is placed in) are added to this basic structure to ensure strong adhesion to negatively charged cell membrane.

While the applications of dPGA are demonstrable [19], important questions remain

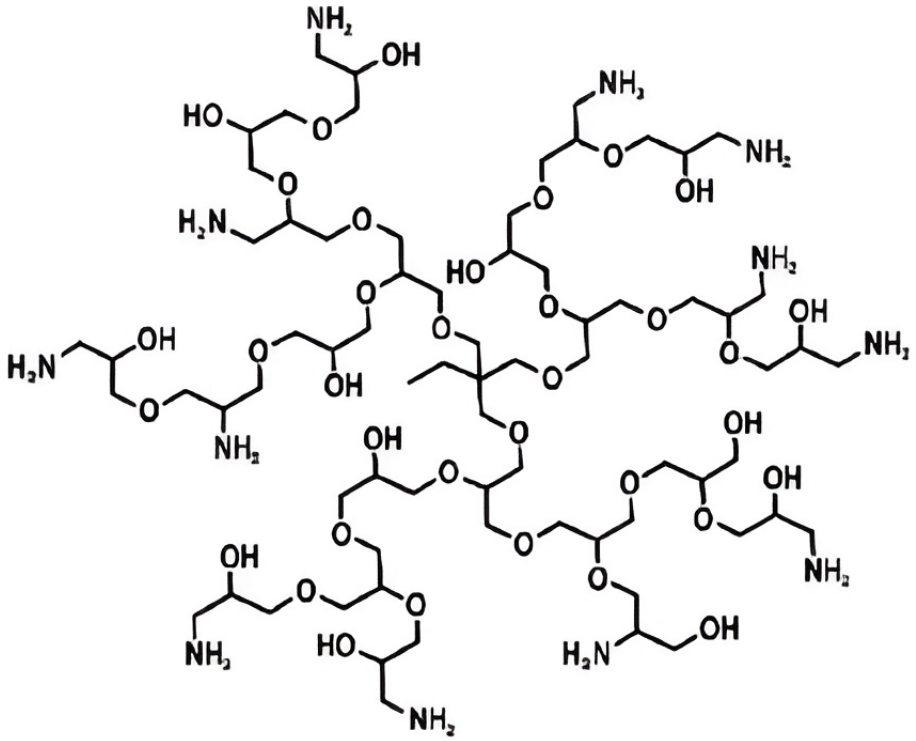

Figure 1.6: Molecular structure of a small dPGA molecule. Following typical chemistry conventions, N represents Nitrogen, O represents Oxygen, OH a Hydroxyl group, and NH_2 an amine group. The unlabelled vertices of the lines between these represent Carbon atoms, and the edges between these vertices represent bonds between atoms. The small Carbon chain at the centre is characteristic of the core of dendrimers created via free-radical polymerization. Taken from [7].

concerning precise characterization of its structure and adsorption behaviour. One Monte Carlo method which has been used successfully in modelling the adsorption process of other polymer coatings such as poly-l-lysine [11] is Random Sequential Adsorption (RSA).

The basic RSA simulation process consists of creating an attempt particle in the shape of a disk at a random location on a 2d surface. If the attempt particle does not intersect with an already placed particle, it is placed itself. If it does, it is rejected and a new attempt particle is created.

By examining the fraction of the surface covered by disks as a function of the number of attempts, an RSA simulation provides a model of the polymer adsorption process from which we can derive information about the speed at which the surface is covered by polymer, the point at which clutter from already placed molecules causes the surface to become saturated, and the structure of the final adsorption monolayer [12].

In chapter 3 of this thesis, we will examine a novel extension of RSA where instead of attempting to place single particles at each step, we instead place entire coarse grained models of dPGA. The first advantage of this is we obtain a more realistic surface coverage curve as the size of each molecule is better represented, as well as a more realistic picture of the final adsorption monolayer. The second benefit is that we can impose more sophisticated successful adsorption requirements than strict intersection checking, which allow for some degree of intersection and focus in on the amine groups which are the main adsorption mechanism for dPGA. We can then vary parameters such as the fraction of branch ends populated by amine groups to obtain particularly valuable information about how varying the polymerization process affects the ability of dPGA to efficiently coat a surface.

2 Highly-Branched Lattice Trees

2.1 Introduction

Polymers are frequently classified by the manner of chemical reactions used to attach the repeating units - a process labelled as *polymerization*. The type of polymerization can affect a multitude of variables relating to the synthesis of polymers and the properties of the product. Of the latter, a particularly interesting and important property of polymers controlled by their polymerization is the amount of branching occurring in the polymer molecule.

When a polymer is synthesized by a process such as chain-growth polymerization, monomers (the repeating units in polymers) are repeatedly attached to the end of a growing chain, creating long string-like molecules known as linear polymers. However, when lengths of polymers have reactive sites other than the two ends of a string, or involve monomers which have or are made to have more than 2 reactive sites in general, chains of polymer can get attached to the sides of each other causing the phenomena of branching.

Depending on the particularities of the polymerization process, branching can occur to a greater or lesser degree, greatly affecting the properties of the produced polymer. To characterize this, chemists examine a quantity called the degree of branching of polymers, which is mathematically defined by (1.1), and extended to lattice trees as in Figure 2.1.

Some well studied classes of polymers with a high degree of branching are hyperbranched polymers, which are synthesized via condensation reactions of AB_2 monomers (monomers including one copy of a particular functional group and two copies of another functional group), dendrimers, which are highly symmetric spherical polymers with many identical branches, and dendrons, which are similar to dendrimers but wedge-shaped. Many other classes of high degree of branching polymers are variations or combinations of these structures.

Hyperbranched polymers have been found experimentally to have a degree of branching typically ranging between $0.4 - 0.6$ [25], and dendrimers have a degree of branching close to or equal to 1. Linear polymers consisting of n monomers will have a degree of branching given by $2/n$, approaching 0 as the size of the polymer increases.

The definition of degree of branching admits an obvious purely graph theoretic inter-

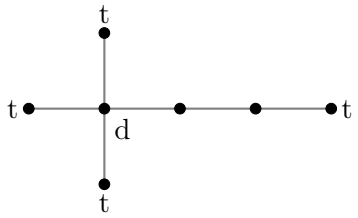

Figure 2.1: Representing a polymer as a graph, this polymer has 4 terminal vertices (labelled by t) and 1 dendritic vertex (labelled by d), giving it $DB = \frac{5}{7}$.

pretation, in which the condition for dendritic and terminal monomers is interpreted in terms of the degree of vertices. This allows for the study of properties of highly branched polymers which are independent of the particular monomers composing them, as well as allowing for making contact with existing work of combinatorial models of polymers which have a general tree shape.

In section 2.2, basic definitions and results of lattice trees are recalled, and HB (highly branched) trees are introduced as a subclass of lattice trees in which the degree of branching is greater than 0.5. Basic lower and upper bounds are introduced, followed by a proof of supermultiplicativity of the number of HB trees of a fixed number of vertices, and a stronger lower bound for HB trees contained in a box.

In section 2.3, adsorption properties of HB trees on an impenetrable surface are studied. The existence of a finite limiting free energy for adsorbing HB trees is shown, and, similarly to known results for lattice trees, the limiting free energy is shown to be equal to the logarithm of a limit of the number of HB trees for certain values of adsorption fugacity, and the location of the critical point for an adsorbed-desorbed phase transition is also shown to be bounded below by the inverse of this limit.

2.2 Definitions and Properties of HB trees

We first recall basic definitions and results concerning lattice trees; a more detailed treatment along with proofs can be found in [21]. A lattice tree is a connected and acyclic graph in the hypercubic lattice $\mathbb{Z}^d$, which has vertices being points in $\mathbb{Z}^d$ and possible edges between vertical or horizontal neighboring points. Important sub classes of lattice trees include so called *star polymers*, consisting of a single central vertex with up to $2d$ branches or linear polymers (i.e. self-avoiding walks) attached to it, *comb polymers* consisting of a

linear polymer 'backbone' with branches attached along one direction, and *brush polymers* consisting of a linear polymer backbone with branches attached along multiple directions. In the rest of the paper, we will be concerned only with lattice trees in $\mathbb{Z}^2$ and neglect to write dimensions. We will make use of the following lemma:

Lemma 2.1. (Fekete's lemma) Let $S \subset \mathbb{N}$ be a semigroup with respect to addition and $(a_n)_{n\in S}$ a sequence of real numbers such that $a_n + a_m \geq a_{n+m}$ for any $m, n \in S$ (i.e. (a_n) is subadditive). Then $\lim_{n\to\infty} \frac{1}{n} a_n = \inf_{n\geq 1} \frac{1}{n} a_n$.

Proof. See [21] A.1. □

Let t_n denote the amount of lattice trees containing N vertices up to translational equivalence. This is known to be supermultiplicative as a function of n [21], i.e. $t_n t_m \leq t_{n+m}$. Another useful fact is that there exists a constant $C > 0$ such that $t_n \leq C^n$ for all $n \in \mathbb{N}$ (in fact this holds for all connected lattice subgraphs, not necessarily acyclic, the class of which is called lattice animals). By taking $-\log$ of t_n we obtain a subadditive sequence, whence it follows from these facts and Fekete's lemma that there exists $\lambda < \infty$ such that

$$\lim_{n\to\infty} \frac{1}{n} \log t_n = \log \lambda \tag{2.1}$$

exists.

We say that τ is an HB (Highly Branched) tree if equation (1.2) holds. This definition also makes sense (both mathematically and from the chemistry perspective) when τ is a lattice tree in 3 dimensions: the definitions of D_d, D_t, D, and DB are not changed. For convenience we will restrict ourselves to $\mathbb{Z}^2$, with all the results below being quite straightforwardly generalizable to the three-dimensional case.

We denote the amount of HB trees with n vertices, considered up to translational equivalence, by h_n. It is easily seen that $h_2 = t_2, h_3 = t_3, h_4 = t_4$, but a linear tree with 5 vertices is not HB, so $h_5 < t_5$. By the same consideration, we have for $n > 4$ an obvious upper bound of $h_n < t_n$, from which we also get from $t_n \leq a_n$ that $h_n < a_n$ where a_n is the number of lattice animals (connected subgraphs of $\mathbb{Z}^2$).

Proposition 2.2. There exists some constant $0 < C < \infty$ such that such that $h_n \leq C^n$ for $n \in \mathbb{N}$.

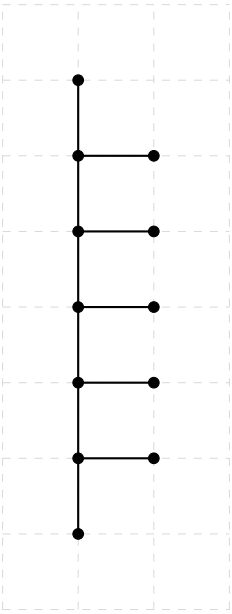

Figure 2.2: Example of a lattice comb with a 7 vertex backbone and 5 teeth.

Proof. As mentioned earlier, this is known for t_n, and $h_n < t_n$. □

A basic lower bound for h_n is given by the following

Proposition 2.3. A comb with a length N backbone is a HB tree if it has at least $\frac{1}{4}N - 1$ non-backbone branches.

Proof. We take a comb to be a linear tree (called the backbone) with edges (called teeth) attached to the inner vertices of the backbone which each make one of the backbone vertices dendritic and add a terminal vertex - see Figure 2.2 for an example. Then the proposition follows from solving $\frac{2+2g}{N} \geq 0.5$ for g, representing the sum of the contribution to the degree of branching from the two terminal vertices of the comb backbone and the contribution of one terminal vertex and one dendritic vertex for each of the g branches attached to one side of the backbone. □

Proposition 2.4. For N even, $2^{N/2+1}\binom{N-2}{N/2} \leq h_{N+1+N/2}$, and for N odd, $2^{N/3+1}\binom{N-2}{\lfloor N/3 \rfloor} \leq h_{N+1+\lfloor N/3 \rfloor}$. It also holds asymptotically that:

$$\frac{(N-2)^{(N-2)/N}}{(\frac{N}{2})^{1/2}(N-2-N/2)^{(N-4)/2N}} \leq \zeta^{3/2}$$

where $\zeta := \lim_{n\to\infty} h^{1/n}$. The existence of this limit will be proved in Theorem 2.7.

Proof. Consider a length N backbone with $N/2$ or $N/3$ branches. Then the inequality of Prop 2.3. is satisfied. Considering comb backbones as sequences of N edges in the same direction, there are 2 distinct possibilities of N edge backbones up to translation, along with $2^{N/2} \cdot \binom{N-2}{N/2}$ or $2^{N/3} \cdot \binom{N-2}{N/3}$ ways of attaching the appropriate number of branches, representing the possible choices of which side of the backbone to attach each branch and the possible choices of re-arranging the branches.

The second inequality follows from taking N-th roots of $2^{N/2} \cdot \binom{N-2}{N/2}$ and applying Stirling's approximation $m! \sim_{m>>1} (m/e)^m \sqrt{2\pi m}$ (where the square root factor is neglected in the asymptotic limit as other factors grow exponentially) to the lower bound for even N.

□

We next turn to a supermultiplicativity proof, which will allow us to later apply Fekete's lemma indirectly, or directly apply a generalization of it [24] for supermultiplicative functions to acquire a limiting growth constant. This is a well-established fact for general lattice trees, and the proof also involves construction of a $1-1$ function as here [21].

Theorem 2.5. The function $f(n) = h_{n-2}$ is supermultiplicative, i.e. $f(n)f(m) \leq f(m+n)$.

Proof. We will prove the equivalent statement that $h_n h_m \leq h_{n+m+2}$ by constructing a $1-1$ map taking ordered pairs of trees from h_n and h_m into h_{m+n+2}.

Let H_1 be a HB tree with n edges and H_2 an HB tree with m edges. Let v_1 be the greatest vertex site of H_1 under the order $(x_1, y_1) > (x_2, y_2)$ if $y_1 > y_2$ or both $y_1 = y_2$ and $x_1 > x_2$, and let v_2 be the greatest vertex site of H_2 under the order $(x_1, y_1) > (x_2, y_2)$ if $y_1 < y_2$ or both $y_1 = y_2$ and $x_1 > x_2$. Note that these are two orders which, colloquially, pick out the 'top-right' vertex of H_1 as v_1 and the 'bottom-right' vertex of H_2 as v_2.

Translate H_1 so that v_1 is at a fixed location (a, b) on the lattice. Next translate H_2 so that v_2 is one step above v_1, $v_2 = v_1 + (0, 1)$. Then attach three edges: an edge connecting v_1 and v_2, an edge connected to the right of v_1 parallel to $\overrightarrow{e_1} = (1, 0)$, and an edge connected to the right of v_2 parallel to $\overrightarrow{e_1}$. See Figure 2.3. for an example of this construction. This creates a tree with $m + n + 2$ vertices, which has 2 new terminal vertices, loses at most 2 terminal vertices, and changes 2 existing vertices into dendritic vertices. Then, denoting the sum of dendritic vertices and terminal vertices in H_1 and H_2 by δ_1, δ_2 respectively, we

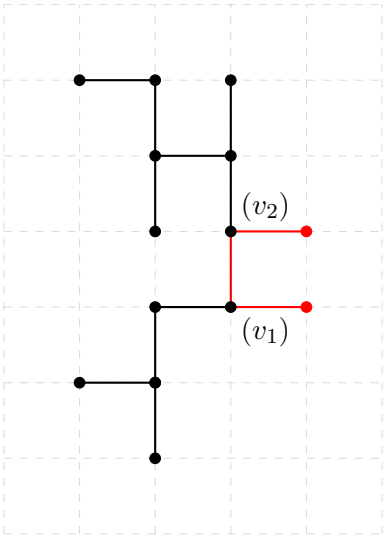

Figure 2.3: Example of concatenation of 2 HB trees as described in Thm 2.5.

have that

$$\frac{\delta_1 + \delta_2 + 2}{n + m + 2}$$

is greater than or equal to $\frac{1}{2}$ from the fact that by assumption

$$\frac{\delta_1}{n} \geq \frac{1}{2} \text{ and } \frac{\delta_2}{m} \geq \frac{1}{2}.$$

Finally we note that this construction indeed provides a $1-1$ map since the trees H_1 and H_2 can be unambiguously recovered by identifying the unique (as guaranteed by the construction) integer s such that the half space defined $y \leq s$ contains $n+1$ edges. As $v_1 = (a, b)$, this integer will be b, and a will be the second largest integer such that (a, b) is in the half-space. We can then remove the edge attaching (a, b) to $(a, b+1)$ and the edges attached to $(a+1, b)$ and $(a+1, b+1)$ to recover H_1 and H_2.

We can then remove the vertices and edges to the right of a and take H_2 to be the tree above $(a, b) + (0, 0.5)$ and H_1 the tree below $(a, b) + (0, 0.5)$. □

Theorem 2.6. There exists a constant $\zeta > 0$ such that

$$\lim_{n\to\infty} \frac{1}{n} \log h_n = \sup_{n>1} \frac{1}{n} \log h_{n-2} = \log \zeta.$$

and this constant is finite by Prop 2.3.

Proof. By the previous theorem, $f(n) = h_{n-2}$ is supermultiplicative, so $-\log(h_{n-2})$ is a subadditive function, hence we can apply Fekete's lemma to it from which the result follows immediately. □

Besides the degree of branching, another frequently studied structural quantity of polymers is the *radius of gyration*, referring to the root-mean square distance of monomers from the centre of mass in a polymer molecule. This gives a measure of the extent to which monomers are congregated around a single point and the radius of this congregation. The following theorem relates to the radius of gyration by giving a lower bound on the number of distinct HB trees which it is possible to fit into a certain radius (considered as a square box) around the origin. The form of this bound and technique of proof does not appear to have been investigated before even for general lattice trees.

Theorem 2.7. Let $||x||$ be the norm on $\mathbb{Z}^2$ defined by $||x|| = \max(|x_1|, |x_2|)$ for a point $x = (x_1, x_2)$.

(1) A lower bound for the number of distinct HB trees of distance $N+1$ from the origin under this norm is given by:

$$(1-2^{-4})^{-3}2^{3N-1}(1-2^{-4\lfloor\frac{3N+4}{8}\rfloor})^3 \text{ for N odd}$$
$$(1-2^{-4})^{-3}2^{3N-4}(1-2^{-4\lfloor\frac{3N+4}{8}\rfloor})^3 \text{ for N even.}$$

(2) Under the same norm, a lower bound for the number of distinct HB trees of distance $5K$ from the origin, for $K \in 3\mathbb{Z}$ greater than 2, is given by:

$$(1-2^{-4})^{-2K-1}2^{5K^2+5K-11}(1-2^{-4\lfloor\frac{15K+4}{8}\rfloor})(1-2^{-4\lfloor\frac{15K-10}{16}\rfloor})^{2K}.$$

In $\mathbb{Z}^3$ with $||x|| = \max(|x_1|, |x_2|, |x_3|)$, we have analogously

(3) A lower bound for the number of distinct HB trees of distance $N+1$ from the origin under this norm is given by:

$$(1-2^{-4})^{-3N}2^{3N^2-N}(1-2^{-4\lfloor\frac{3N+4}{8}\rfloor})^{3N} \text{ for N odd}$$
$$(1-2^{-4})^{-3N}2^{3N^2-4N}(1-2^{-4\lfloor\frac{3N+4}{8}\rfloor})^{3N} \text{ for N even.}$$

(4) Under the same norm a lower bound for the number of distinct HB trees of distance $5K$ from the origin, for $K \in 3\mathbb{Z}$ greater than 2, is given by:

$$(1-2^{-4})^{-2K^2-K}2^{5K^3+5K^2-11K}(1-2^{-4\lfloor\frac{15K+4}{8}\rfloor})^K(1-2^{-4\lfloor\frac{15K-10}{16}\rfloor})^{2K^2}.$$

Proof. We begin by considering the two dimensional case. Consider 3 kinds of 'moves' in which one can concatenate steps starting from the origin. These are:

- l_k - two steps in the $k-$th cardinal direction
- c_{kj} - one step in the $k-$th cardinal direction followed by one step in the $j-th$ direction (which we constrain to be a direction orthogonal to k)
- t_{kji} - one step in the $k-$th direction followed by simultaneous steps in the two directions orthogonal to it, forming a 'T' shape.

The strategy of this proof will be to consider the contribution to $wt = D_d+D_t-D_x$ of each move, where D_x is the amount of vertices which are not dendritic or terminal, and consider how many of the N-length combinations (which will have length N under the norm in the statement of the theorem) of these moves will yield a HB tree. Evidently, an $N-$length string of such moves will be a distance N away from the origin with respect to the max norm, hence the lower bound is given as a function of this distance.

We will restrict ourselves to k being the north direction, as the arguments for k being other directions are identical, and consider moves attached to the highest (most north) vertices of the preceding move. We make the following restriction in how moves can be added (see Fig. 2.4. for clarification):

- Whenever a move follows a c move, it will always be attached to the right vertex of the top row.

There is also ambiguity in how a move can be attached to a t move, as there are 3 possible ways of doing so, but in every case, assuming that each move has moves preceding and following it (ignoring the terminal vertices of the tree for now), we see that that in the 'worst' case (with respect to positive changes in the value of wt) l always contributes a factor of -1 to the quantity wt by adding one vertex in D_x, c contributes a factor of -2,

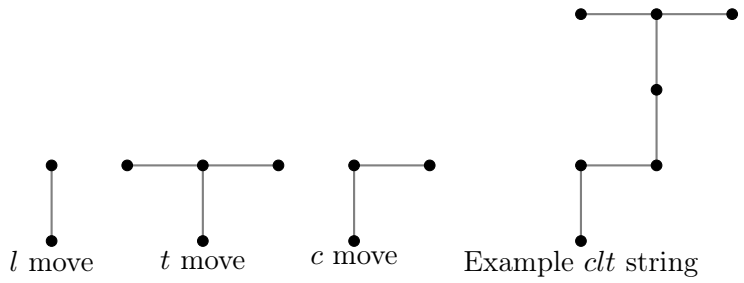

Figure 2.4: Graphs of the 3 moves as well as one example of a string.

and t contributes a factor of at least +2 by adding a dendritic vertex and a terminal vertex to the tree.

Consider strings of length N. We will consider the amount of possible HB strings of length N given a fixed amount of c moves in the string. This means solving the system

$$\begin{aligned} 2t - 2c &\geq \frac{N}{2} - 2 \\ c + t &= N \end{aligned} \tag{2.2}$$

where the -2 term arises from each string having a minimum 2 terminal vertices, and we exclude the possible l term as we are only concerned with the maximum possible c moves for an HB string to be possible, hence we look at the maximum possible contribution to wt from the remaining moves in the string, which comes from t moves. The solution $c \leq \frac{3N+4}{8}$ implies that there can be HB strings of length N whenever there are less than $\frac{3N+4}{8}$ 'c' moves in the string.

Each of these strings will have $N - R$ combinations of t and l moves, where R denotes the amount of c moves. We then calculate the amount of ways of choosing t and l moves such that the string is HB. To do this we first solve

$$\begin{aligned} t + l &= N - R \\ 2t - l &\geq \frac{N}{2} + 2R - 2 \end{aligned} \tag{2.3}$$

whence we have that the string is HB when $l \leq \frac{N}{2} - \frac{4}{3}R + \frac{2}{3}$. Combining this with the solution of (2.3), we have a lower bound for the number of HB length N strings given by

$$\sum_{R=0}^{\frac{3N+4}{8}} \sum_{k=0}^{\frac{N}{2}-\frac{4}{3}R+\frac{2}{3}} \binom{N-R}{k}.$$

To ensure the sum is well-defined and for access to a convenient binomial coefficient summation formula, we will instead examine the smaller quantities

$$\begin{gathered}\sum_{R=0}^{\lfloor\frac{3N+4}{8}\rfloor}\sum_{k=0}^{\frac{N-4R-1}{2}}\binom{N-4R}{k} \text{ for } N \text{ odd and} \\ \sum_{R=0}^{\lfloor\frac{3N+4}{8}\rfloor}\sum_{k=0}^{\frac{N-4R-2}{2}}\binom{N-4R-1}{k} \text{ for } N \text{ even.}\end{gathered} \tag{2.4}$$

for N even. We then utilize the well known binomial coefficient identity

$$\sum_{i=0}^{\frac{P-1}{2}}\binom{P}{i} = 2^{P-1} \text{ for P odd}$$

followed by the usual geometric series partial sum formula to acquire

$$\begin{gathered}(1-2^{-4})^{-1}2^{N-1}(1-2^{-4\lfloor\frac{3N+4}{8}\rfloor}) \text{ for N odd} \\ (1-2^{-4})^{-1}2^{N-2}(1-2^{-4\lfloor\frac{3N+4}{8}\rfloor}) \text{ for N even.}\end{gathered} \tag{2.5}$$

We then repeat this construction two more times in the directions orthogonal to the first tree by means of the following construction (see Fig. 2.5. for clarification).

Firstly, translate the tree above one step in the north direction, and attach a step connecting the bottom of the tree to the origin. Then we attach two edges to the origin in the east and west directions, and attach another tree built by the same procedure, but in the west direction, to the right end of the east edge and another tree built by the same procedure but in the east direction to the left end of the east edge. To ensure this newly constructed tree is HB, we also attach to the bottom of it two downwards steps with two steps attached to the right and left vertices of the sites created by the downwards steps. In combination with the extra vertex at the origin, this construction removes 3 terminal vertices from the trees attached to it, creates a dendritic vertex at the origin, creates two dendritic vertices and four terminal vertices from the edges attached below the origin, and adds 7 vertices total. Hence it causes a net change of +4 to δ (recall that δ is the sum of the number of dendritic and terminal vertices) and adds 7 vertices to the union of 3 copies of the original tree, and thus is HB.

This cubes the lower bound of (4.4), and then the result follows by noting we can repeat

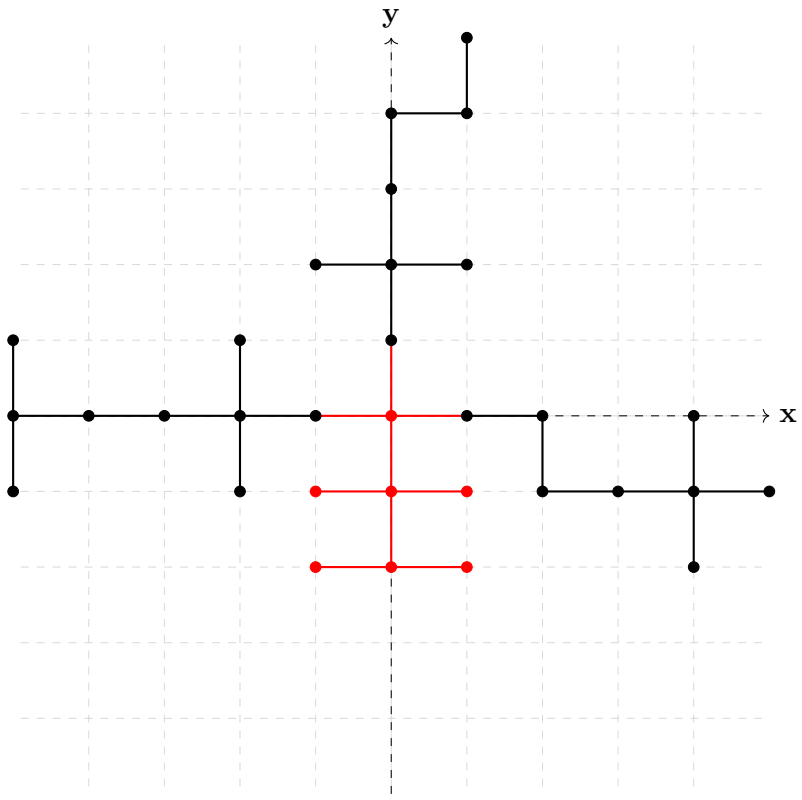

Figure 2.5: Example of combination of 3 strings (the subtrees in black) as described in Thm 2.7

the entire above construction in the same manner in each of the 4 cardinal directions.

For part (2), first note in a c move the horizontal edge in the j direction in the step can be moved 1 unit in the $-j$ direction so that it is attached to the left of the upper vertex of the other edge, and moves following a t move can be taken on either of the vertices at the ends of the edges in the j direction. This implies that any string of length N can be taken to lie in a rectangle of height N vertices and width 5 vertices, which we will then assume for the following.

Translate the box given by the vertices of distance $5K$ so that the bottom of it lies along the origin, and attach a string constructed in the same manner as described above to the origin going upwards in the positive y direction. On the line at $y = 3$, we will attach additional strings to the vertex with the smallest x coordinate and the vertex with the greatest x coordinate. To do this, attach to the rightmost $y = 3$ coordinate an edge in the positive x direction creating another vertex w, attach to w another edge above or below w parallel to the y direction depending on which site is open (at least one must be open by how the string is constructed), attach another edge in the positive x direction to w creating

a new vertex a, attach an edge below or above a, and then, finally, attach the additional string to a. The same process is applied, mutatis mutandis, to the leftmost $y = 3$ coordinate.

We repeat this for the vertices on the lines $y = 5K$. Each attached string produces a factor of the form (2.5) with $\frac{5K-9}{2}$ substituted in for N. The number $\frac{5K-9}{2}$ comes from the remaining length for the string to traverse in the box, minus a 2 from the 4 edge construction taking up a length of 2 added when attaching it. Thus the bound takes the form

$$(1-2^{-4})^{-1}2^{5K-1}(1-2^{-4\lfloor\frac{15K+4}{8}\rfloor})[(1-2^{-4})^{-1}2^{\frac{5K-9}{2}-1}](1-2^{-4\lfloor\frac{15K-10}{16}\rfloor})]^{2K}$$

which simplifies to the stated bound. Bounds (3) and (4) apply from repeating this construction for every plane $Z = a \in \mathbb{Z}$ in the three-dimensional box.

□

Lastly we have monotonicity results:

Theorem 2.8. For h_n the number of HB trees with n sites, we have that $h_n \leq h_{n+2}$ and $h_n \leq h_{n+3}$.

Proof. Let τ be a tree in h_n and w the greatest vertex of τ with respect to y coordinate or with respect to x coordinate if there are multiple vertices with the highest y coordinate, which is then necessarily of degree 1 or 2. Attach one edge to the top of w parallel to $\overrightarrow{e_2} = (0,1)$ and two edges to either side of the newly created vertex parallel to $\overrightarrow{e_1} = (1,0)$. This creates 3 new vertices, adds two terminal vertices and at least one dendritic vertex, and possibly removes a terminal vertex. Thus it increases $\delta = D_t + D_d$ by at least 2 and v by 3, thus creating a tree in h_{n+3}. The original tree τ can be uniquely recovered by removing all vertices with the highest y coordinate and all edges they are attached to.

Again let τ be a tree in h_n and w the greatest vertex of τ under the same order. Attach one edge to the top of w parallel to $\overrightarrow{e_2}$ and one edge to the right side of w parallel to $\overrightarrow{e_1}$. This creates two new vertices, and adds two terminal vertices, one dendritic vertex, and potentially removes one terminal vertex. Thus it increases δ by at least 2 and v by 2, and hence gives a tree in h_{n+2}. The tree τ can be uniquely recovered by removing the vertex with the highest y coordinate and the edge it's attached to, and removing the vertex one step below in the $-e_2$ direction and to the right in the e_1 direction and the edge it's attached to. □

2.3 Adsorption Properties

The degree of branching of a polymer has been shown experimentally to have some correlation with the degree of adsorption in hyperbranched polymers [3], likely due to the increased amount of functional groups on terminal units of the polymer allowing for adsorption reactions.

Mathematically, the general setup for considering adsorption of lattice trees is to take a hyperplane within the hypercubic lattice $\mathbb{Z}^d$ to be the (impenetrable or penetrable) 'surface', and then to consider some manner of energy incentive or disincentive for sites of the tree lying on the surface and study the resulting partition function and the corresponding free energy (e.g. [14]).

In the context of this paper, we will consider the impenetrable surface defined by the vertical line $x = 0$ in the plane. Let $\mathcal{H}_n$ be the set of all HB trees with n sites/vertices, one of which is the origin, let $\overline{\mathcal{H}}_n$ be the set of equivalence classes under translation along the y direction of $\mathcal{H}_n$, and let $\mathcal{H}_n^+$ be the set of trees in $\mathcal{H}_n$ for which all sites (x_1, y_1) have $x_1 \geq 0$. It follows immediately from the definitions of these classes that

$$|\overline{\mathcal{H}}_n| \leq |\mathcal{H}_n^+| \leq |\mathcal{H}_n|. \tag{2.6}$$

We then consider the partition function

$$Z_n(\beta) = \sum_{\tau \in \mathcal{H}+} e^{\beta(\sigma(\tau))}. \tag{2.7}$$

β is the adsorption fugacity, representing the energetic favourability of adsorption, and is in general a function of the Gibbs energy of adsorption. $\sigma(\tau)$ is a function counting the number of sites of τ which lie along $x_1 = 0$ (e.g. in the tree τ of Figure 1.5 $\sigma(\tau) = 2$), which we will sometimes refer to as simply adsorbed sites.

Theorem 2.9. For $\beta < \infty$, the limit

$$\mathcal{F}^{\mathcal{H}+}(\beta) = \lim_{n \to \infty} \frac{1}{n} \log Z_n(\beta).$$

exists and is non-decreasing, convex, continuous, and differentiable almost everywhere.

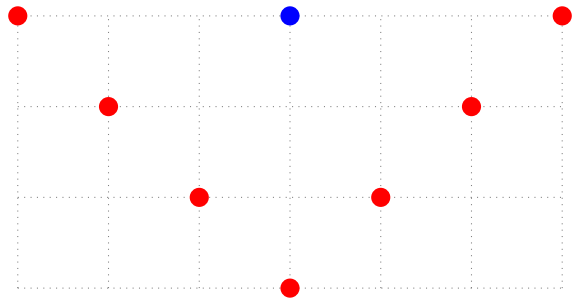

Figure 2.6: The blue dot represents v_1 from the proof of Theorem 2.10, and the red dots represent possible locations of v_2.

Proof. Let $H_1 \in \mathcal{H}_n^+$ and $H_2 \in \mathcal{H}_m^+$. We perform the following 2 steps:

1. Translate H_1 in the y direction until the y coordinate of the bottom vertex of H_1 is 3 steps greater than the y coordinate of the top vertex of H_2.

2. Translate H_1 in the negative y direction until a vertex of H_1 can be reached in 3 steps from a vertex of H_2.

We will first show that after the two above steps, H_1 and H_2 can be connected to make a new tree in H_{n+m+4}^+. Call the referenced vertex of H_1 in step (2) v_1 and the referenced vertex of H_2 v_2. In Fig. 2.6. the blue vertex represents v_1 and the red vertices the possible locations of v_2. Other locations of v_2 are precluded by step (2) stopping translation immediately when vertices are within 3 steps of each other appear.

In Fig. 2.7. we display corresponding possible paths connecting H_1 and H_2. Once each path is created, we can then add two additional edges two it (drawn in blue). That there is space for these two edges to be added for at least one of these paths is in each case guaranteed by step (2): if the space taken by a blue vertex were already occupied, the translation process would have terminated sooner.

With these two blue edges added, we then examine the DB in the newly joined tree made by creating a path as in Fig. 2.7. joining H_1 and H_2, which we will call H_{12}. Creating a path between v_1 and v_2 removes up to 2 terminal vertices if both v_1 and v_2 happen to be terminal vertices. The path created between H_1 and H_2 adds 4 vertices to H_{12}. Because of the blue edges in these paths, two of these vertices are dendritic, and two of these vertices are terminal. Hence in creating H_{12} we have removed up to 2 terminal vertices, added 4 vertices, added 2 dendritic vertices, and added 2 terminal vertices, so that in the limiting

case we have

$$\frac{\delta_1 + \delta_2 - 2 + 2 + 2}{m+n+4} = \frac{\delta_1 + \delta_2 + 2}{m+n+4} \geq \frac{1}{2}$$

by H_1 and H_2 being HB.

Next, to show that this construction maps pairs from $\mathcal{H}_n^+$ and $\mathcal{H}_m^+$ to $\mathcal{H}_{n+m+4}^+$ in a $1-1$ manner, let w_1 be the lexicographically greatest vertex lying along the surface $x = 0$ in H_{12}, and w_2 be the lexicographically smallest vertex lying along the surface $x = 0$ in H_{12}.

After the above construction, we can find a unique path P of edges connecting w_1 to w_2 in H_{12}. As this path will pass through the 3 steps added to adjoin H_1 and H_2, there will be at least one edge we can remove from the path to obtain two unattached trees of size $m+2$ and $n+2$. By ensuring that H_1 in the above construction always has less than or equal the amount of vertices as in H_2, then if we are travelling along P beginning from w_1, the first edge where we can do this will always be the second of the three edges used to attach H_1 and H_2. Call this removed edge e. If e_1, e_2 were the two vertices of e, then remove the four edges connected to e_1 and e_2, and the original trees are then recovered: the tree containing w_1 must be H_1 and the tree containing w_2 must be H_2 since w_1 cannot travel below w_2 in the steps (1) and (2) above.

With this in hand, we have

$$Z_n(\beta)Z_m(\beta) = \sum_{\tau \in \mathcal{H}_n^+} e^{\beta\sigma(\tau)} \sum_{\tau' \in \mathcal{H}_m^+} e^{\beta\sigma(\tau')} = \sum_{\tau,\tau'} e^{\beta(\sigma(\tau)+\sigma(\tau'))}$$

from which we get

$$Z_n(\beta)Z_m(\beta) \leq \sum_{\tau \in \mathcal{H}_{n+m+4}^+} e^{\beta\sigma(\tau)} = Z_{n+m+4}(\beta)$$

up to a constant factor of e^{β} or $e^{2\beta}$ due to the above construction of H_{12} potentially creating new vertices along $x_1 = 0$, causing $\sigma(H_{12}) > \sigma(H_1) + \sigma(H_2)$. However this finite constant can be factored out of limits, so we can apply the Wilker-Whittington generalized supermultiplicative function theorem [24] to obtain the result. □

With this result in hand, we then follow the argument given in [14] to establish the form of $\mathcal{F}^{\mathcal{H}_+}(\beta)$. First we note that there is a $1-1$ map of trees in $\mathcal{H}_{n-3}^+$ to trees τ in $\mathcal{H}_n^+$ with

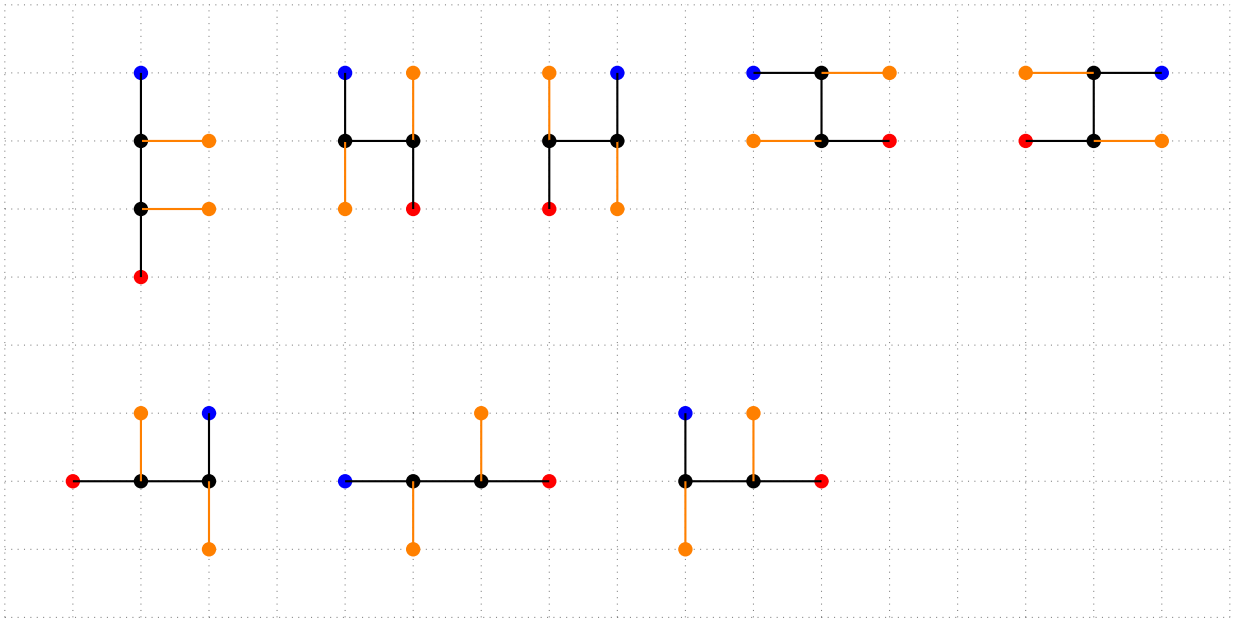

Figure 2.7: Possible paths between the blue vertex and red vertices in Fig. 2.5., corresponding to v_1 and v_2 in the proof of Thm. 2.11. The black vertices and edges display the path added to connect v_1 and v_2, and the orange edges and vertices show the additional edges connected to this path to ensure the constructed tree is HB.

$\sigma(\tau) = 1$ obtained by translating trees in $\mathcal{H}^+_{n-3}$ two steps to the right, attaching two steps to connect the tree to the origin, and then attaching a third step upwards to the middle vertex of the just added two steps (see Fig. 2.8.).

The resulting tree is HB since the construction adds at least one dendritic vertex and one or two more terminal vertices while only adding three additional vertices, and the map is $1-1$ since the mapped tree can be unambiguously recovered by reversing the steps above. This along with (2.7) then gives us the lower bound

$$h_{n-3}e^{\beta} \leq Z_n^{\mathcal{H}+}(\beta). \tag{2.8}$$

Then, if $\beta \leq 0$, we note that we also have (by the definitions of $\mathcal{H}^+_n$ and $\overline{\mathcal{H}}_n$)

$$Z_n^{\mathcal{H}+}(\beta) \leq |\mathcal{H}^+_n| \leq nh_n \tag{2.9}$$

Applying logarithms and limits, it then follows from (2.9) and (2.10) that, when $\beta \leq 0$

$$\mathcal{F}^{\mathcal{H}+}(\beta) = \log(\zeta). \tag{2.10}$$

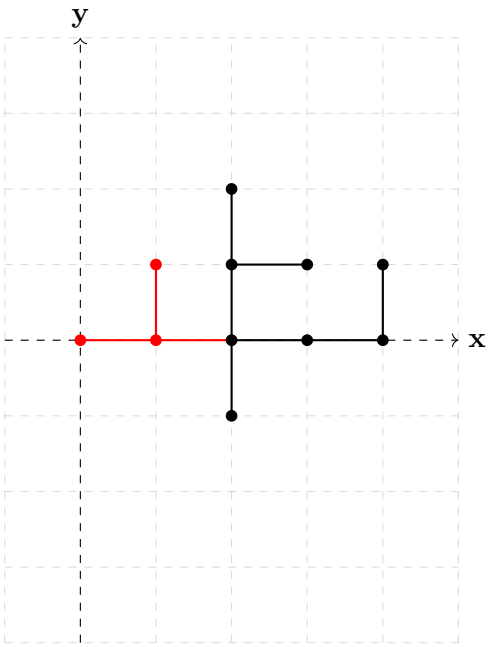

Figure 2.8: Example extension of an HB tree in $\mathcal{H}_8^+$ to an HB tree τ in $\mathcal{H}_{11}^+$ with $\sigma(\tau) = 1$.

As ζ is constant, (2.10) implies $\mathcal{F}^{\mathcal{H}+}(\beta) = \mathcal{F}^{\mathcal{H}+}(0)$ for $\beta \leq 0$, implying that when the adsorption fugacity is negative (i.e. the surface is repulsive to the polymer) the free energy of adsorption is negligible. The next theorem describes at what value of β the transition occurs from this state to one in which there is a significant free energy reward for adsorption. The fact that such a transition occurs also requires the following argument. Consider an HB tree with $N/2$ adsorbed sites (for instance a comb with backbone perpendicular to $x = 0$ and $N/2$ teeth), whence we can pull out a single term from the partition function to have the inequality

$$Z_n(\beta) > \exp(\frac{N}{2}\beta) \tag{2.11}$$

and from taking logs we have

$$\log Z_n(\beta) > \frac{N}{2}\beta \tag{2.12}$$

which implies that $\mathcal{F}^{\mathcal{H}+}(\beta)$ cannot be constant for all values of β.

Theorem 2.10. $\mathcal{F}^{\mathcal{H}+}(\beta) = \log \zeta$ for $\beta \leq \zeta^{-2}$.

Proof. The following proof proceeds identically to theorem 2.1. of [14] up to the construction of the $1-1$ map f, which is necessarily different in our case to account for the HB condition.

For convenience we repeat the steps of the proof preceding the construction of f here as well.

First, we define $l_n(k) = |\{\tau \in \mathcal{H}_n^+ : |\sigma(\tau)| = k\}|$, which is non-zero by definition of the class $\mathcal{H}_n^+$, and which gives us

$$|\mathcal{H}_n^+| = \sum_{k=1}^{N} l_n(k) \tag{2.13}$$

which we can substitute into the partition function to get

$$Z_n^{\mathcal{H}+} = \sum_{k=1}^{n} l_n(k) e^{\beta k}. \tag{2.14}$$

Expanding e as a power series then gives

$$Z_n^{\mathcal{H}+} = \sum_{k=1}^{n} \sum_{j=0}^{\infty} \frac{\beta^j k^j}{j!} l_n(k). \tag{2.15}$$

Next we apply the inequality

$$\frac{k^j}{j!} \leq \binom{k+j-1}{j}. \tag{2.16}$$

The expression on the right side of this inequality describes the amount of $k-$ tuples of non-negative integers which sum to j. To make use of this interpretation, we define a weighted HB tree to be an HB tree $\tau \in \mathcal{H}_n^+$ which has a non-negative integer weight $w(\tau; v)$ assigned to each adsorbed site. Then if $\mathcal{H}_n^{(j)}$ is the set of all weighted trees with N sites and total weight j, we have from the above discussion

$$|\mathcal{H}_n^{(j)}| = \sum_{k=1}^{n} \binom{k+j-1}{j} l_n(k). \tag{2.17}$$

and combining the above 3 equations gives

$$Z_n^{\mathcal{H}+}(\beta) \leq \sum_{j=0}^{\infty} \beta^j |\mathcal{H}_n^{(j)}|. \tag{2.18}$$

Next we attempt to find an upper bound for $|\mathcal{H}_n^{(j)}|$ by constructing a $1-1$ map $f : \mathcal{H}_n^{(j)} \to \mathcal{H}_{n+2j}$. Let $\tau \in \mathcal{H}_n^{(j)}$.

Let v be an adsorbed site in τ, and suppose there are no other adsorbed sites with non zero weight within 1 step of v. Then if $w(\tau; v) = q$, we attach q iterations to the left of v

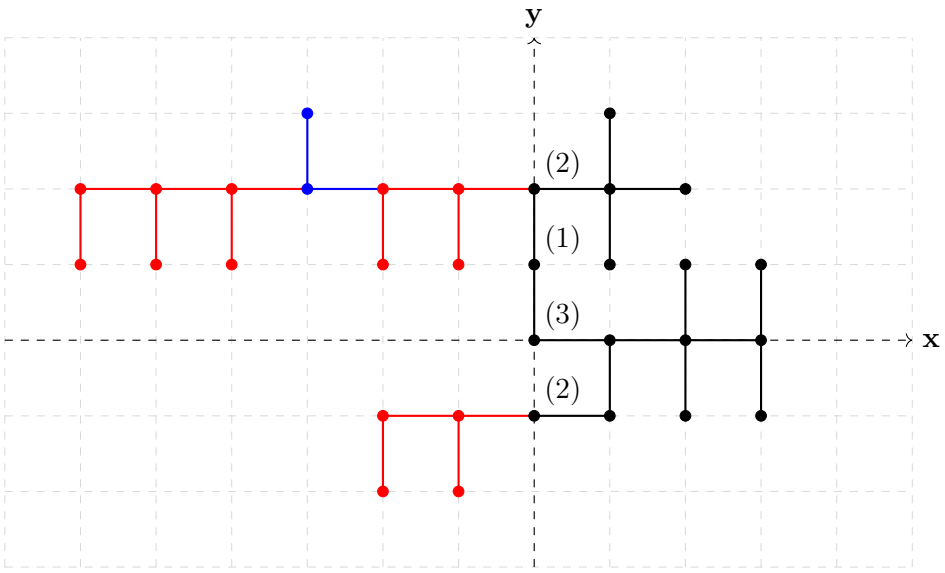

Figure 2.9: Example of the construction described in the proof of Theorem 2.11. The black edges and vertices form the initial weighted tree, and the coloured edges and vertices show the construction attached to the no longer weighted tree under the mapping of f. In the higher attachment of coloured edges, we have $v = (0,2), r = (0,1), m = (0,0), p = 2, q = 1$, and $x = 3$..

of taking 1 step to the left and attaching 1 edge downwards to the newly created vertex. If there is 1 other adsorbed site r within 1 step of v with non-zero weight, then suppose without loss of generality r has a greater y-coordinate than v. If $w(\tau; r) = q$ and $w(\tau; v) = p$, we attach to the left of r q iterations of the same construction as in the previous case, and we then also attach p iterations of the same construction but with the downwards edge attached to each step replaced with an upwards edge (see figure for clarification). Next suppose there are 3 adsorbed sites with non zero weight within 2 steps of each other, call them v, r, m with weights p, q, x respectively. Then we attach the same construction as above to the highest of the 3 adsorbed sites p times with a downwards edge, q times with an upwards edge, and x times again with a downwards edge (see Figure 2.9.).

Then, if we have a sequence of more than 3 vertices with non zero-weight each within 1 step of each other, we apply the latter construction (for 3 vertices of non-zero weight together) to the top 3 vertices, apply it again to the next 3 vertices below them, and so on until there are 2 vertices left in which case we apply the two vertex construction, 1 vertex left in which case we apply the one vertex construction, or no vertices left.

This then creates a tree with $n+2j$ sites, which is HB since each addition of the iterated construct adds at least one terminal vertex and two vertices total, and the above rules for

the construction of this tree ensure it is $1-1$ mapping of $\mathcal{H}^{(}j)_n$. Applying the definition of the codomain of f then gives us the upper bound

$$|\mathcal{H}_n^{(j)}| \leq (n+2j)h_{n+2j}. \tag{2.19}$$

Applying this to eq 2.17 and using that $(h_n \leq \zeta^N)$ by theorem 2.6. above then gives

$$Z_n^{\mathcal{H}+}(\beta) \leq \sum_{j=0}^{\infty}(n+2j)\beta^j\zeta^{n+2j} = \frac{n\zeta^n}{1-\beta\zeta^2} + \frac{\zeta^n(\beta\zeta^2)}{(1-\beta\zeta^2)^2} \tag{2.20}$$

From adding together the fractions we find this expression is less than or equal to

$$\frac{n\zeta^n}{(1-\beta\zeta^2)^2} \tag{2.21}$$

and applying $\lim_{n\to\infty}\frac{1}{n}\log$ gives

$$\begin{aligned}
&= \lim_{n\to\infty}\frac{1}{n}[\log(n\zeta^n) - \log(1-\beta\zeta^2)^2] \\
&\leq \lim_{n\to\infty}\frac{1}{n}(\log(n) + n\log(\zeta) \\
&= \lim_{n\to\infty}\log\zeta = \log\zeta
\end{aligned}$$

Combining this with (2.9) then implies the result. □

3 Random Sequential Adsorption Modelling of dPGA

Random sequential adsorption (RSA) is a simple algorithm for modelling the density and growth of adsorption monolayers. Briefly described in the introduction, we review RSA in more detail here. In its simplest form [9], it models the adsorption process of monodisperse colloidal particles: individual particles are modelled as disks placed flat onto a 2D surface. At each step of the algorithm, an attempt disk is created at a random location on the surface. If it intersects with already placed disks, the attempt disk is rejected. If it does not, the attempt disk is placed on the surface permanently (see Fig. 3.1).

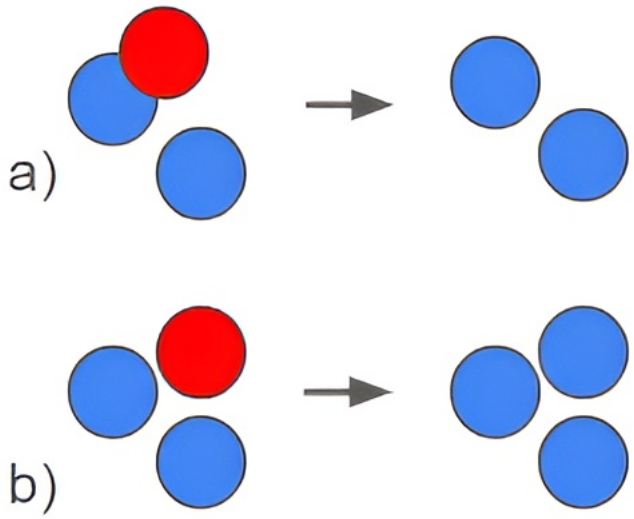

Figure 3.1: Simple 2D RSA scheme step: in a) an attempt disk (red) intersects with already placed disks (blue) and is rejected. In b) it does not intersect with already placed disks, and is added/adsorbed to the surface.

Extensions of RSA to different shapes of basic particles [12], as well as combinations of basic shapes into basic polymer structures [6] have also been studied.

From an RSA simulation, we can determine at each step the coverage fraction θ, defined by

$$\theta = N\frac{A_P}{S} \tag{3.1}$$

where N is the amount of placed particles, A_p the area of the kind of particle being used,

and S the area of the surface on which they are placed. In an RSA simulation, θ can be graphed as a function of the amount of attempts (successful or unsuccessful) in a simulation τ by computing the value of θ in Eq. (3.1) after each attempt. Figure 3.2 gives an example plot of θ against τ in a simple (2D simulation with circular disks) RSA simulation.

When θ reaches a sufficiently large value θ_∞, called the *jamming coverage*, the surface is saturated with particles so that no more successful attempts are possible. For the above described 2D disk RSA model, the jamming coverage is known to be 0.547. From RSA simulation we obtain information about how quickly a surface is saturated with adsorbent, when such saturation occurs, and a visualization of the adsorbed monolayer during the various times of the adsorption process.

3.1 Basic dPGA RSA Algorithm

Here we consider an extension of the above RSA model for dPGA. The dPGA molecule consists of a hyperbranched polyglycerol structure with some fraction of the branch ends populated with amine groups. In solution, these amine groups pick up positive charges and provide a mechanism for the dPGA molecule to strongly adsorb to negatively charged cell membranes.

To better connect with this structure, we modify the above RSA algorithm in two ways. Firstly, instead of placing individual disks onto the surface, we attach disks together to build a dendrimer structure (see Fig. 3.3.), and place these dendrimers onto the surface. Secondly, instead of checking for intersection at every disk, we randomly select 50% of the outermost disks of an attempt dendrimer and check for intersection between these selected discs and any of the discs from already placed dendrimers. Other RSA treatments of dendrimers (e.g. [5]) typically focus on placing single disks as in typical RSA with the diameter of each disk matched to that of the average adsorbed dendrimer, and incorporate more sophisticated effects (such as the electrostatic interactions from protonated amino groups) via adding potential functions (such as screened Coloumb force) which increase or decrease the effective radius of each disk. The approach taken here allows us to study the impact of varying parameters relating to the structure and composition of the dendrimer.

Tthe steps of the modifed RSA algorithm during each attempt are as follows:

Basic dPGA RSA Algorithm

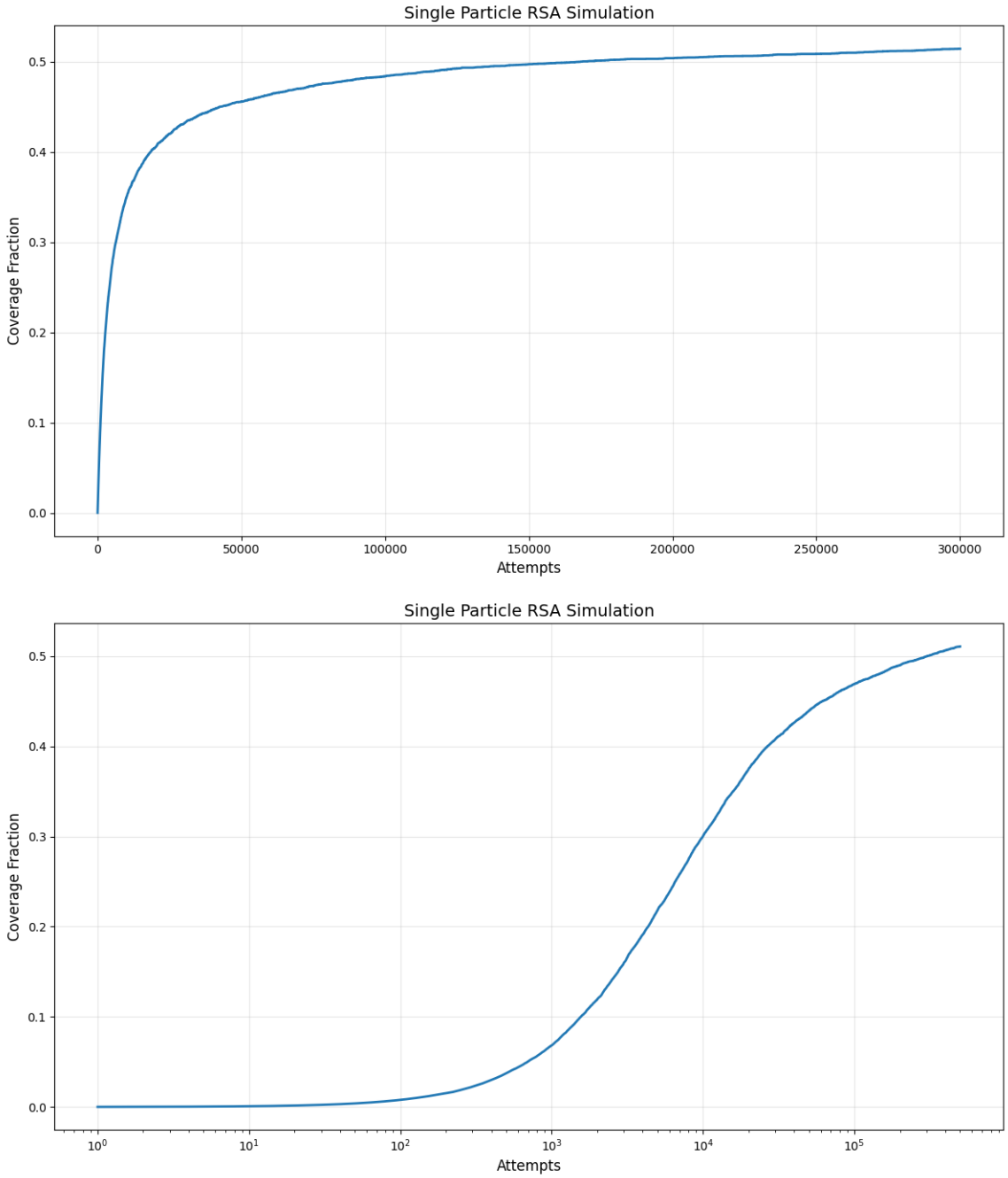

Figure 3.2: Example plots of surface coverage fraction against amount of attempts in a basic single particle RSA simulation. Both plots contain the same information, but the logarithmic scale (bottom) is typically preferred by experimentalists.

1. A single 'core' disk is created at a random location on the surface.

2. Three more disks are attached to this core disk at random angles. If the attached disks intersect, the attempt is rejected.

3. Two disks are attached to each of the previously attached three disks at random angles. If the attached disks intersect with already placed disks, the attempt is rejected.

4. The previous step is repeated g times with respect to the most recently attached generation of disks, where g is the desired total number of generations.

5. Once g generations have been added, half of the outermost disks are selected and stored as 'B-disks'.

6. If any of the B-disks intersect with any disks of already placed dendrimers, the attempt dendrimer is rejected. If none of the B-disks intersect with any disks of already placed dendrimers, the attempt dendrimer is placed.

In Fig. 3.4 we show an example of the coverage fraction over time during a simulation run of the preceding algorithm. Note that due to allowing for intersection between the disks that are not B-disks when placing new dendrimers (as we only check for intersection at the B-disks), it is possible for the coverage fraction θ, as calculated by (3.1), to exceed 1 in this algorithm as A_p is computed as the sum of the areas of all disks within each dendrimer. Hence θ in this algorithm gives some measure of the 3-dimensional structure of the monolayer rather than simply the fraction of the area covered, in the sense that the areas of each overlapping dendrimer contributes to θ. Unsurprisingly, coverage fraction curves resulting from this algorithm show a steeper initial increase compared to the basic colloidal RSA model, and have significantly higher values of θ_∞.

3.2 Modified dPGA RSA Algorithm

We consider two modifications to the above algorithm - one minor and one moderate. In the first, we change the fraction of B-disks attached to the end groups of each dendrimer. Physically, this corresponds to varying the fractions of end groups populated by amine groups, which can occur as a result of variability in synthesizing the molecule. Under the assumptions of the basic dPGA RSA algorithm, dendrimers which have fewer B-disks

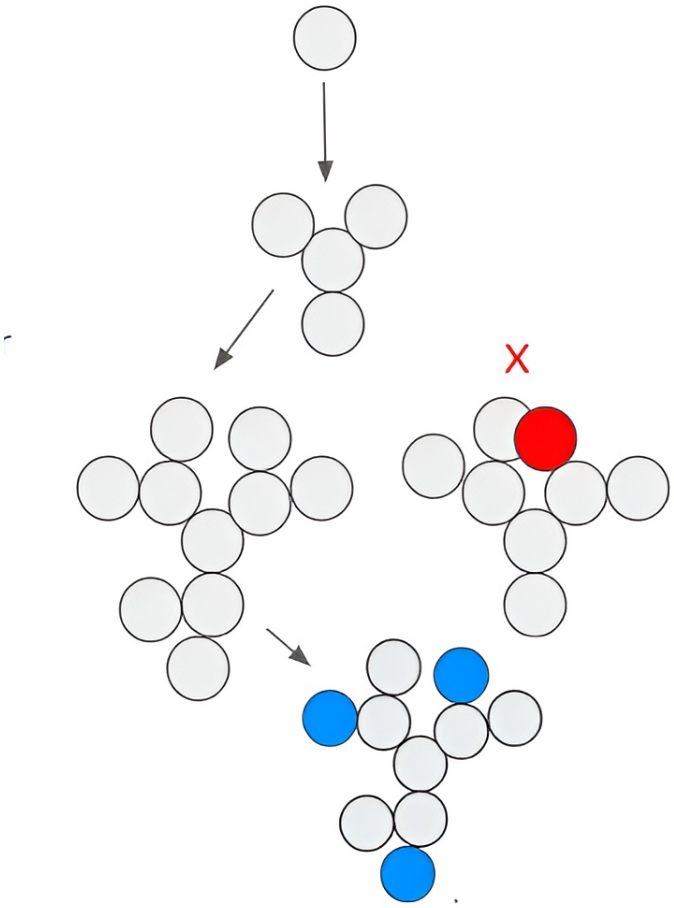

Figure 3.3: A dendrimer is built by first placing a single disk (top), attaching 3 more disks to it for the initial branches, and then attaching 2 more disks to each outer disk until a sufficient number of generations are added. Disks are not allowed to intersect while building the dendrimer. Once the dendrimer has reached sufficient size, half of the outer disks are randomly selected as 'B-disks' (blue).

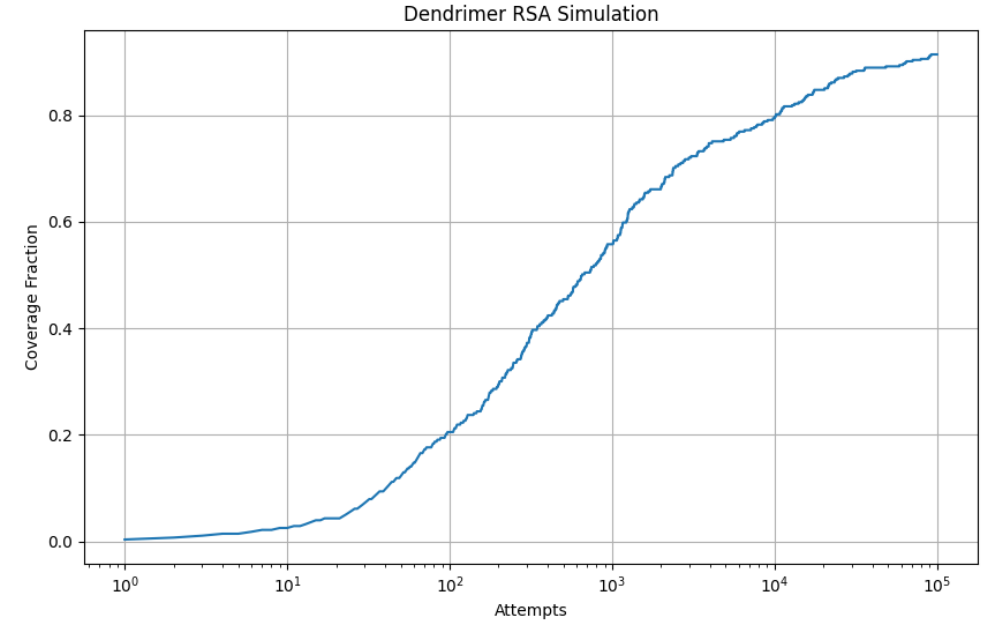

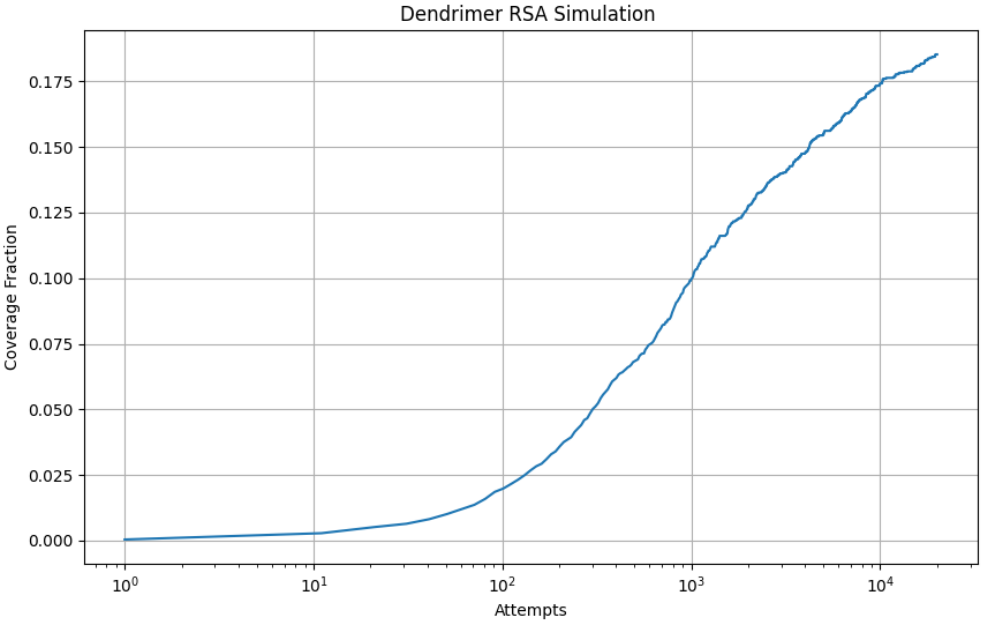

Figure 3.4: The above image is an example plot of surface coverage fraction θ calculated according to Eq. (3.1.) against the amount of attempts in a basic dPGA RSA algorithm simulation.The lower image is another plot of the basic dPGA RSA algorithm, with surface coverage calculated according to amount of surface covered by dendrimers over total area rather than θ (i.e. we do not add the areas of all disks of adsorbed dendrimers, we only look at the area of surface covered by them, so there is no multiple-counting from overlapping dendrimers).

groups will have an easier time successfully adsorbing to the surface due to having fewer possible ways of intersecting with already placed dendrimers. This is indeed reflected in the simulation data, and manifests itself in the coverage fraction curves beginning to diverge from each other once the possibility of intersection starts to become non-trivial (Figure 3.5).

In the second modification considered of the basic dPGA RSA algorithm, we adopt a more flexible methodology of creating dendrimers and checking their intersection. Firstly, when building dendrimers, we allow the branches being constructed to overlap with each other.

In the 2-dimensional RSA model, the model dendrimers can be thought of as projections down to the surface of the actual 3-dimensional molecules, in which case overlapping branches would correspond to the tangling and overlapping of branches in an actual dendrimer structure. Hence the self-intersection simplification in this model is less adequate for smaller dendrimers or dendrimers which adsorb strongly enough to a surface that they become largely flat.

When a dendrimer is successfully placed, we compute and record the convex hull spanned by all of its B-disks. When a new attempt dendrimer is made, instead of checking intersection with every already placed disk, we check intersection of attempt dendrimer B-disks with all convex hulls of already placed dendrimers.

Instead of rejecting an attempt dendrimer if any of its B-disks intersect with any convex hulls, we specify some threshold $K \in (0, 1]$ of allowable intersection fraction. That is, if the amount of attempt dendrimer B-beads intersecting with placed dendrimer convex hulls divided by the total amount of attempt dendrimer B-beads exceeds K, the attempt dendrimer is rejected. Otherwise it is successfully placed.

This allows for enabling a controlled degree of overlap behaviour between adsorbed dendrimers, which makes the simulation produce more realistic behaviour of the adsorbed monolayer. An example of the results using this convex hull modification is given in Figure 3.6.

3.3 Comparison to Data

To apply the above models to experimental data on dPGA, we firstly determine a disk size via molecular dynamics, as there are currently no direct experimental measurements

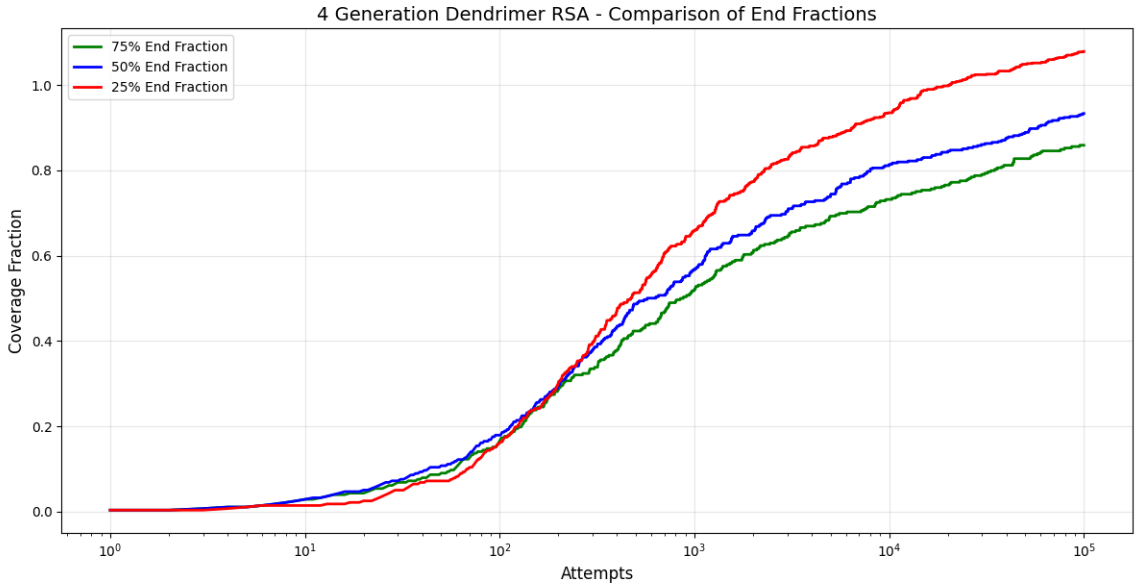

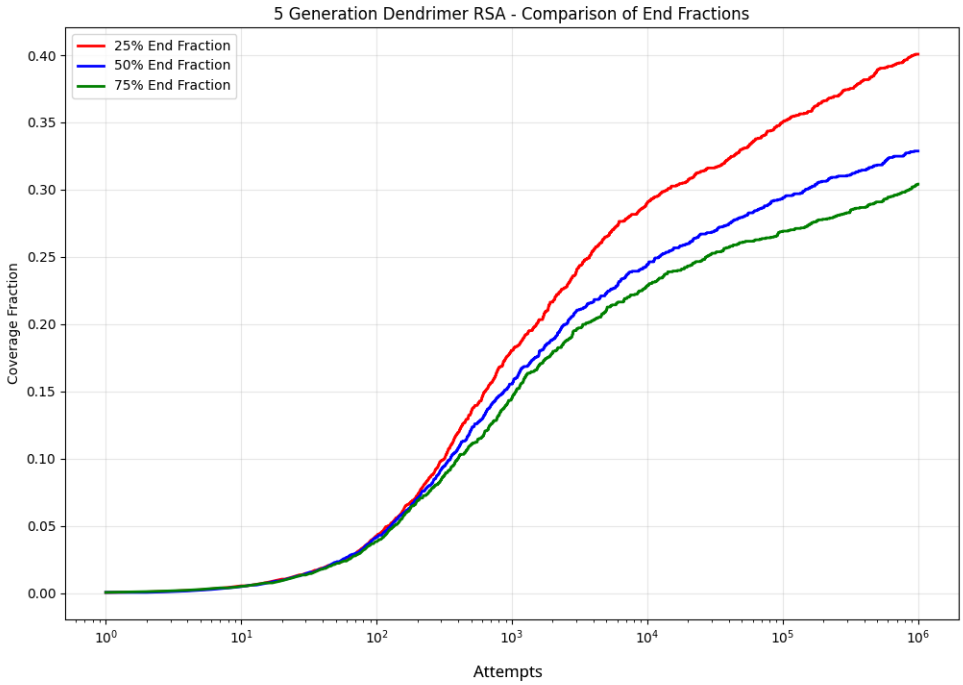

Figure 3.5: The upper image is an example plot of surface coverage fraction against amount of attempts in a modified dPGA RSA algorithm simulation with varying fraction of B-disks on the branch ends. The lower image is another example plot of the first modification dPGA RSA algorithm, with surface coverage calculated according to amount of surface covered over total area rather than θ.

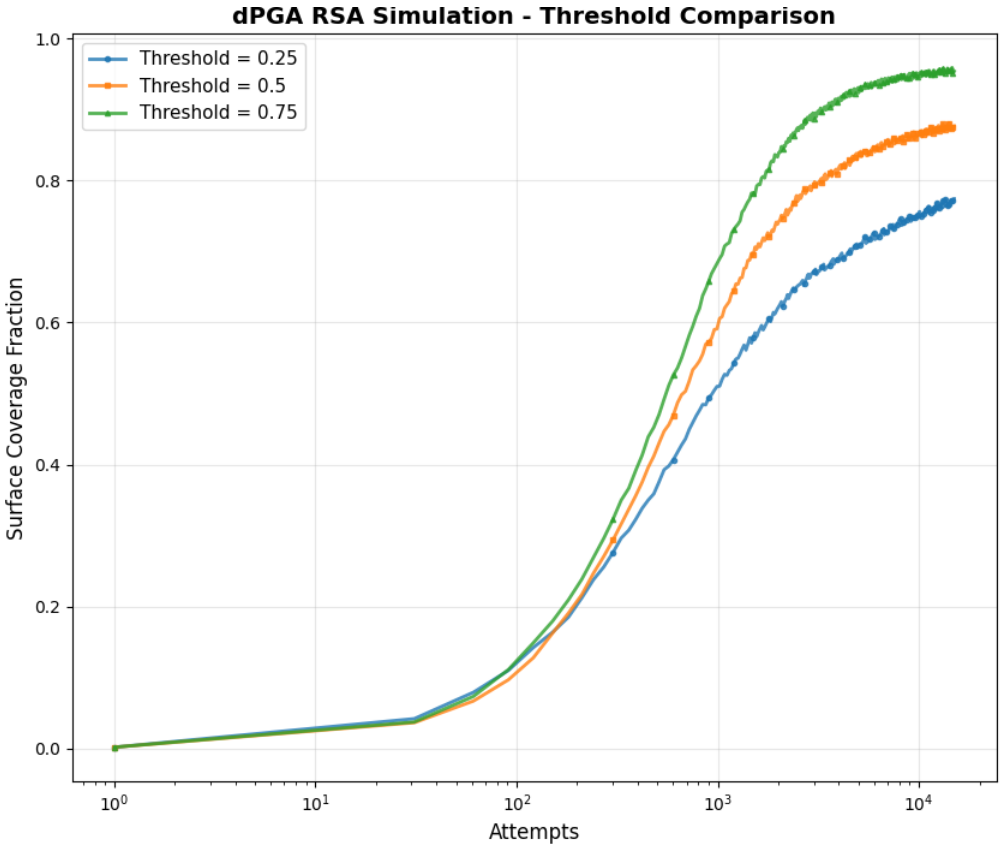

Figure 3.6: An example plot of the second modification considered in section 3.2. of the dPGA algorithm at different intersection threshold (defined as K above), with surface coverage fraction calculated by amount of area covered over total area.

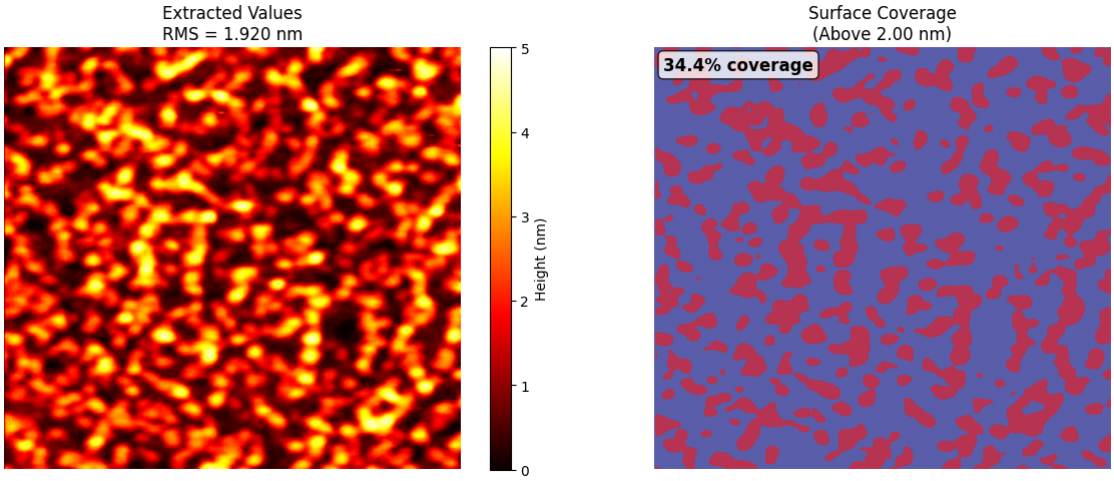

Figure 3.7: On the left is an AFM image of a dPGA monolayer after thirty seconds coloured with respect to height. On the right, a filter has been applied to display pixels of the image with a height over 2nm in red, from which surface coverage can be measured (0.344 in this example). This image and the ellipsometry data below are displayed with permission from the McGill University Barrett Research Group.

of the size of dPGA or its monomers. Molecular dynamics is a method of 'brute forcing' dynamical behaviour of a molecule by setting up all the equations of motion for the structure and size of all the constituent parts of a molecule (e.g. bond length, bond angle, particle location) and solving them numerically [13]. Unfortunately little work has been done on generating paramater sets (called "force fields") for these equations of motion, but some success has been found with general force fields [16] which are used here.

The dynamics of a small dPGA molecule during 50ns in solution was simulated in GROMACS with the CHARMM force field and xtb with the GFN-FF [18] force field. The average size of monomers was then measured after the molecule was dynamically simulated, yielding an average length of 4.72 angstrom which was then used as the initial diameter of the dendrimer RSA disks.

Next, to compare the surface coverage predicted by RSA simulations to empirical data, firstly a measure of surface coverage was taken from AFM images of dPGA by extracting the surface area above a height threshold of 2nm to measure the area of adsorbed dPGA (Fig 3.7.).

As a monolayer, it can be roughly assumed that the surface coverage over time during the adsorption process is proportional to the film thickness, which was measured via ellipsometry methods. Then we can normalize the ellipsometry data so the peak thickness has the same

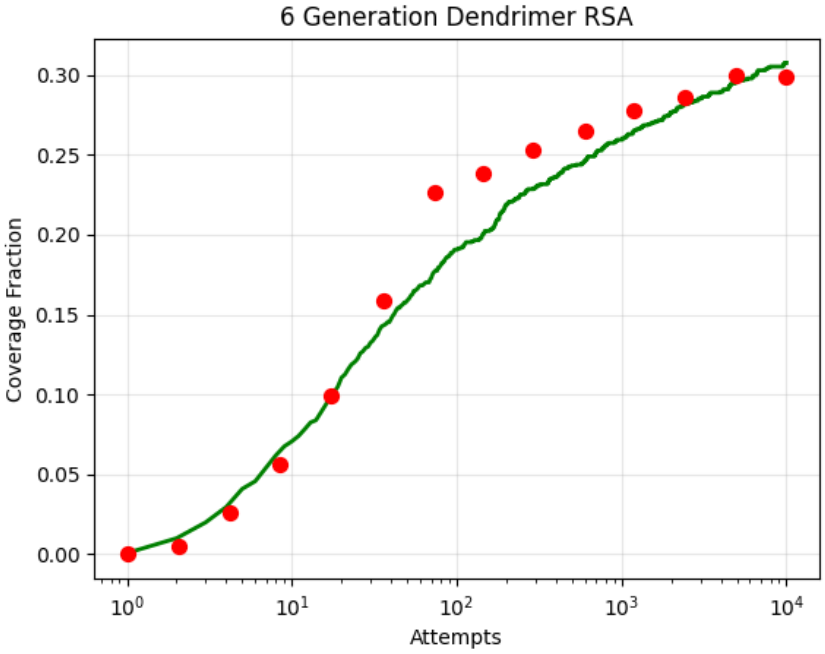

Figure 3.8: A plot of the first modification dendrimer RSA simulation (green) with normalized ellipsometry data superimposed (red points).

numerical value as the surface coverage after the surface is saturated.

The surface coverage fraction after 30s of adsorption was measured to be approximately 0.3 (Fig. 3.7.). This matches well with the saturation surface coverage of the first modification dendrimer RSA with 4 generations and 50% end fraction simulation, allowing for a comparison as in Fig. 3.8.

Fitting this data by varying the generations of dendrimers in the RSA simulation and the bead diameter also allows us to vary the fraction of B-beads at the end of the dendrimer to see how surface coverage varies as a function of amination (Fig. 3.9).

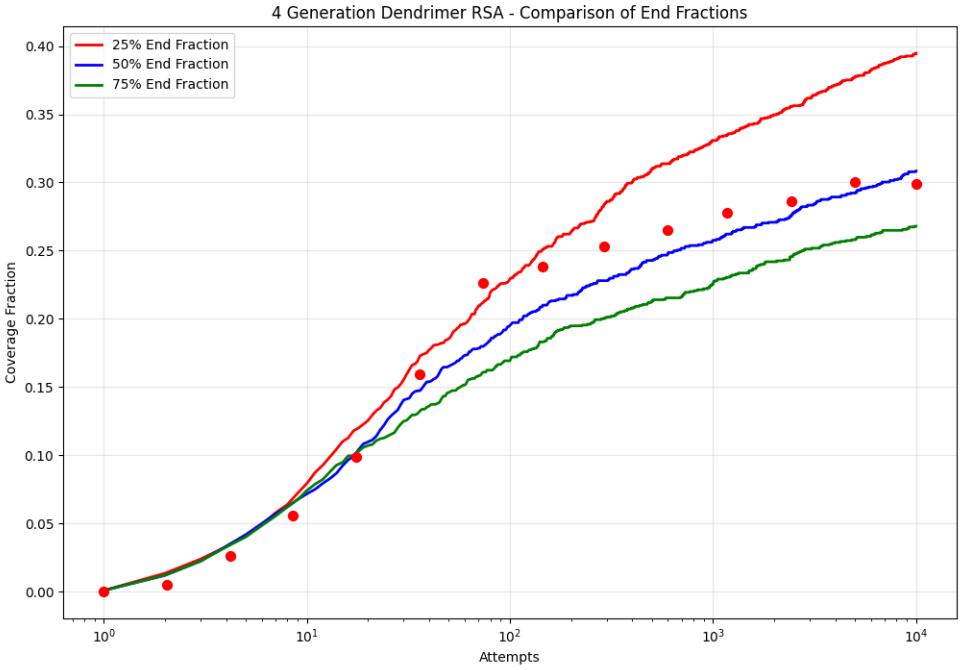

Figure 3.9: A plot of the first modification dendrimer RSA simulation with varying branch end B-disk fractions (using the same parameters as in Figure 3.8 for the 50% fraction curve) with normalized ellipsometry data superimposed.

4 Conclusion and Discussion

The results in chapter 2 show that frequently studied limits for general lattice trees such as $\lim_{n\to\infty} \frac{1}{n} \log t_n$ and $\lim_{n\to\infty} \frac{1}{n} \log Z_n(\beta)$ exist for HB trees as well, along with associated constants. What was not established, however, is any information on how these constants for HB trees differ from those for general lattice trees. In fact, little information at all about how HB trees differ from general lattice trees was established beyond the rather trivial observation that $h_n \leq t_n$. Analytical results about the differences between HB trees and general lattice trees is obstructed by the difficulty of finding exact results about the latter, which does not become significantly easier for HB trees.

An easier approach to comparing the two is via Monte Carlo simulation for numerical results. Sampling high numbers of lattice trees with various numbers of vertices using the algorithm of [22], no significant differences were found in well-studied quantities such as span, radius of gyration, and length of longest path between HB trees and general lattice trees. Additionally, these quantities generally did not show any significant correlation with the degree of branching.

Here the distinction between the coarse modelling of polymers by lattice trees and actual polymers should be kept in mind. The polymers for which chemists make use of the degree of branching are not random configurations of monomers and bonds, but products of particular polymerization processes with certain stochastic kinetics that produce variation in branching in different samples. It is between such different samples that the degree of branching can usefully highlight differences, and not between samples of two arbitrarily different species of polymer.

Hence while there are still huge swaths of results still open for HB trees beyond what was done in this thesis, it may be more interesting (and easier) to apply combinatorial methods to trees constrained to have some particular architecture or to have been built according to some particular kinetic process, and then see how DB constraints and predictions behave among these classes of polymer models.

The modified Random Sequential Adsorption modelling of chapter 3 was used successfully to interpret and extrapolate from experimental results on dendritic Polyglycerol Amine,

and indeed the modifications of the model were made with the adsorption process of this specific dendrimer in mind.

Surprisingly, while RSA modelling has been tried for different polymer geometries [6], there does not appear to be any previous work on applying it to the adsorption of branched polymers.

Part of the explanation of this lacuna may be related to the computational difficulties discussed in chapter 3: constructing structures such as dendrimers while avoiding self-intersection results in computationally heavy simulations making it difficult to run simulations for sufficiently long time scales. Allowing for self-intersection, as was done in the modifications presented here, greatly improves computational performance but comes at the cost of making analytical results inaccessible. A variety of formulas for derived quantities and approximations are available for basic single-disk RSA [2] which aid in both fitting and interpretation. This is considerably more difficult for self-intersecting dendrimers due to the variations in area covered by each molecule and variations in the geometry of each molecule.

Further study on dendrimer RSA, or perhaps branched polymer RSA more generally, may be best focused on more extensive simulation to establish quantities like jamming coverage for various different parameters, and for adapting and applying the RSA models here to other situations of interest.

References

[1] Srinivas Abbina et al. “Hyperbranched polyglycerols: recent advances in synthesis, biocompatibility and biomedical applications”. In: *Journal of Materials Chemistry B* 5.47 (2017), pp. 9249–9277.

[2] Zbigniew Adamczyk. *Particles at interfaces: interactions, deposition, structure*. Vol. 20. Elsevier, 2017.

[3] Younes Ahmadi and Ki-Hyun Kim. “Hyperbranched polymers as superior adsorbent for the treatment of dyes in water”. In: *Advances in Colloid and Interface Science* 302 (2022), p. 102633.

[4] Gary A Banker. “Trophic interactions between astroglial cells and hippocampal neurons in culture”. In: *Science* 209.4458 (1980), pp. 809–810.

[5] Brian P Cahill et al. “Adsorption of poly (amido amine)(PAMAM) dendrimers on silica: Importance of electrostatic three-body attraction”. In: *Langmuir* 24.2 (2008), pp. 465–473.

[6] Michał Cieśla. “Continuum random sequential adsorption of polymer on a flat and homogeneous surface”. In: *Physical Review E* 87.5 (2013), p. 052401.

[7] Jean-Pierre Clément et al. “Dendritic polyglycerol amine: an enhanced substrate to support long-term neural cell culture”. In: *Asn Neuro* 14 (2022), p. 17590914211073276.

[8] John M Dealy, Daniel J Read, and Ronald G Larson. *Structure and Rheology of Molten Polymers: From Structure to Flow Behavior and Back Again*. Carl Hanser Verlag GmbH Co KG, 2018.

[9] Jens Feder. “Random sequential adsorption”. In: *Journal of Theoretical Biology* 87.2 (1980), pp. 237–254.

[10] Chao Gao and Deyue Yan. “Hyperbranched Polymers: From Synthesis to Applications”. In: *Progress in Polymer Science* 29.3 (2004), pp. 183–275.

[11] Dominik Kosior et al. “Formation of poly-l-lysine monolayers on silica: Modeling and experimental studies”. In: *The Journal of Physical Chemistry C* 124.8 (2020), pp. 4571–4581.

[12] Piotr Kubala et al. “Random sequential adsorption: an efficient tool for investigating the deposition of macromolecules and colloidal particles”. In: *Advances in Colloid and Interface Science* 306 (2022), p. 102692.

[13] Andrew R Leach. *Molecular Modelling: Principles and Applications*. Pearson Education, 2001.

[14] Neal Madras. “Location of the adsorption transition for lattice polymers”. In: *Journal of Physics A: Mathematical and Theoretical* 50.6 (2017), p. 064003.

[15] Neal Madras and Gordon Slade. *The Self-Avoiding Walk*. Springer Science & Business Media, 2013.

[16] Nuno Martinho et al. “Molecular modeling to study dendrimers for biomedical applications”. In: *Molecules* 19.12 (2014), pp. 20424–20467.

[17] Michael Rubinstein and Ralph H Colby. *Polymer Physics*. Oxford University Press, 2003.

[18] Sebastian Spicher and Stefan Grimme. “Robust atomistic modeling of materials, organometallic, and biochemical systems”. In: *Angewandte Chemie International Edition* 59.36 (2020), pp. 15665–15673.

[19] Louise Thiry et al. “Optimization of long-term human iPSC-derived spinal motor neuron culture using a dendritic polyglycerol amine-based substrate”. In: *ASN neuro* 14 (2022), p. 17590914211073381.

[20] Nicolaas Godfried Van Kampen. *Stochastic Processes in Physics and Chemistry*. Vol. 1. Elsevier, 1992.

[21] EJ Janse Van Rensburg. *The Statistical Mechanics of Interacting Walks, Polygons, Animals and Vesicles*. Oxford University Press, USA, 2015.

[22] EJ Janse Van Rensburg and Neal Madras. “A nonlocal Monte Carlo algorithm for lattice trees”. In: *Journal of Physics A: Mathematical and General* 25.2 (1992), p. 303.

[23] Carlo Vanderzande. *Lattice Models of Polymers*. 11. Cambridge University Press, 1998.

[24] JB Wilker and SG Whittington. “Extension of a theorem on super-multiplicative functions”. In: *Journal of Physics A: Mathematical and General* 12.10 (1979), p. L245.

[25] Deyue Yan, Chao Gao, and Holger Frey. *Hyperbranched Polymers: Synthesis, Properties, and Applications*. John Wiley & Sons, 2011.

[26] Robert J Young and Peter A Lovell. *Introduction to Polymers*. CRC Press, 2011.